

Ultrafast Energy Transfer from a Carotenoid to a Chlorin in a Simple Artificial Photosynthetic Antenna

Alisdair N. Macpherson,^{*,†} Paul A. Liddell,[‡] Darius Kuciauskas,[‡] Dereck Tatman,[‡] Tomas Gillbro,[†] Devens Gust,^{*,‡} Thomas A. Moore,^{*,‡} and Ana L. Moore^{*,‡}

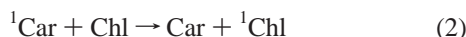
Department of Biophysical Chemistry, Umeå University SE-901 87 Umeå, Sweden, and the Center for the Study of Early Events in Photosynthesis, Department of Chemistry and Biochemistry, Arizona State University, Tempe, Arizona 85287-1604

Received: May 16, 2002

A model photosynthetic antenna system consisting of a carotenoid moiety covalently linked to a purpurin has been prepared to study singlet–singlet energy transfer from a carotenoid to a cyclic tetrapyrrole. Ultrafast fluorescence upconversion measurements of the carotenopurpurin dyad and an unlinked reference carotenoid demonstrate that the fluorescent S_2 excited state of the carotenoid model has a lifetime of 150 ± 3 fs, whereas the corresponding excited state of the carotenoid in the carotenopurpurin dyad is quenched to 40 ± 3 fs. This quenching is assigned to energy transfer from the S_2 state to the purpurin with a $73 \pm 6\%$ efficiency, which is in accord with the $67 \pm 4\%$ quantum yield obtained by steady-state fluorescence excitation measurements. Concomitant with the decay of the carotenoid S_2 excited state, a single-exponential rise of the excited S_1 state of the purpurin moiety was observed at 699 nm with a time constant of 64 fs. However, the decay of the fluorescence anisotropy was faster at this wavelength (40 fs) and isotropic rise times as short as 44 fs were determined at other emission wavelengths. The lifetime of the S_1 state of the carotenoid (7.8 ps) was the same in both the carotenoid model and the dyad. Taken together, these results unequivocally demonstrate that the S_2 state of the carotenoid moiety is the sole donor state in this efficient singlet–singlet energy transfer process. The simple dyad described in this work mimics the ultrafast energy transfer kinetics found in certain naturally occurring pigment protein complexes and is thus able to reproduce the high electronic coupling needed for efficient energy transfer from an extremely short-lived energy donor state.

Introduction

Carotenoids play several roles in the photosynthetic process and are crucial to the photoprotection of photosynthetic membranes.^{1–3} As accessory light-harvesting pigments, carotenoids (Car) are found in the chlorophyll-binding antenna proteins of photosynthetic organisms where they absorb light in the blue-green spectral region and efficiently transfer energy (eqs 1 and 2) to nearby chlorophylls (Chl).



Light energy collected in this way is funneled to reaction centers where energy conversion to electrochemical potential takes place. Carotenoids are known to have at least two low-lying excited singlet states from which energy transfer to chlorophylls (eq 2) could occur. Two of the possible singlet–singlet energy transfer pathways are shown schematically in Figure 1.

Initially, absorption of light by the carotenoid populates the S_2 ($1^1B_u^+$) state (the “forbidden” S_1 state has a vanishingly small absorption coefficient), but rapid internal conversion to the lower-lying S_1 ($2^1A_g^-$) state ensues. Energy transfer from this state to the Q_y (S_1) level of the chlorophyll is one possible

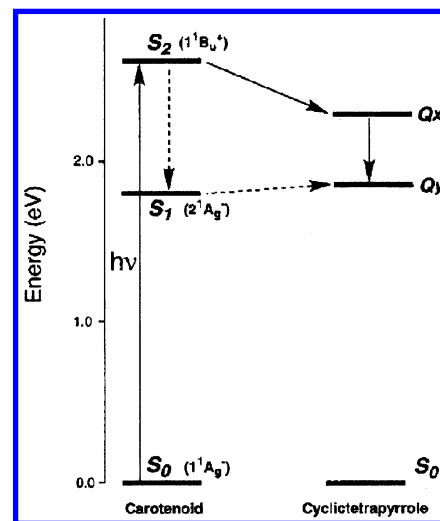


Figure 1. Energy transfer pathways from the carotenoid to the purpurin tetrapyrrole in dyad 1: (—) path involving the S_2 state of the carotenoid; (---) path involving the S_1 state of the carotenoid. Excitation to the S_2 state of the carotenoid is indicated. Note that the energy of the S_1 state is uncertain (see Discussion).

pathway. However, energy transfer from the S_2 state of the carotenoid directly to the Q_x (S_2) state of the chlorophyll, in competition with the ultrafast internal conversion from the S_2 to the S_1 state of the carotenoid, is also feasible. The extremely short lifetime of the S_2 state of the carotenoid (<300 fs) does not a priori exclude this second pathway.⁴ Indeed, the observa-

* Corresponding authors. E-mail: alisdair.macpherson@chem.umu.se, gust@asu.edu, tmoore@asu.edu, amoore@asu.edu.

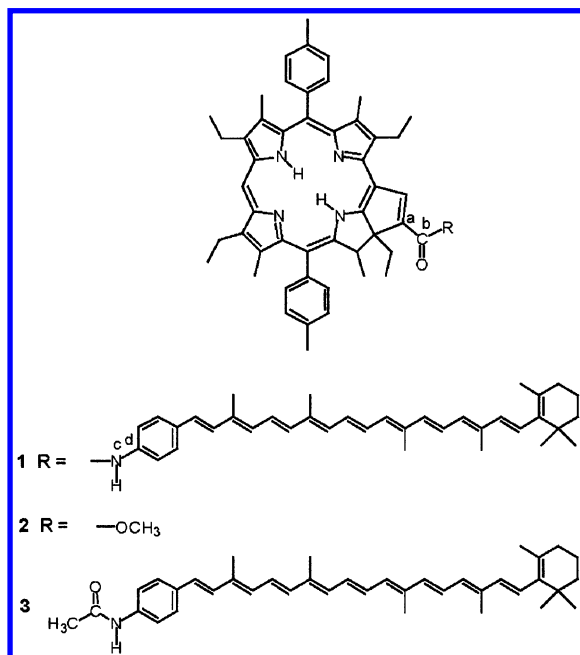
[†] Umeå University.

[‡] Arizona State University.

tion of ultrafast chlorophyll or bacteriochlorophyll rise kinetics (≤ 240 fs) following excitation of the carotenoids in certain photosynthetic light-harvesting complexes suggests that some energy transfer occurs from the carotenoid S_2 state, rather than entirely from the lower energy excited S_1 state, as predicted by Kasha's Rule.^{5–7} Furthermore, two recent ultrafast fluorescence upconversion studies of the peripheral (LH2) antenna complex of purple bacteria conclude that energy transfer from the carotenoids proceeds predominantly from the S_2 state.^{8,9} The complexity of these natural antenna systems containing multiple chromophores, compounded with the ultrafast time scale, inevitably makes detailed pathway assignments very difficult. Mimicking this unusual photophysical behavior in simple, well-defined model systems offers the opportunity to study the energy transfer pathways in detail, and to explore and control the nature of the carotenoid–tetrapyrrole electronic interactions mediating the process.^{8,10} In this work we report the rate, efficiency, and pathway of energy transfer in a carotenopurpurin dyad (**1**) where the two chromophores, carotenoid and tetrapyrrole-macrocycle, are in close proximity and partially conjugated.

Results

Synthesis. The 5,15-diaryloctaalkylporphyrin required for the synthesis of **1** was prepared by the method of Gunter and Robinson,¹¹ with adaptations from Smith et al.¹² A nickel(II)



complex of this porphyrin was formylated and then a Wittig type reaction was carried out to generate a *meso*-2-(ethoxycarbonyl)vinylporphyrin. The cyclization reaction which yielded the purpurin was carried out by refluxing this porphyrin in 1,2-dichloroethane with triethylamine. Hydrolysis of the ester and coupling with 7'-apo-7'-(4-aminophenyl)- β -carotene¹³ were the final steps in the synthesis of **1** (see Experimental Section).

Molecular Conformations. The amide group used as the linker in dyad **1** should preclude large-scale intramolecular motions between the chromophores, constraining the interchromophore separation, angles, and electronic coupling interactions. From molecular modeling (MM2), the distance from the center of the macrocyclic ring to the center of the carotenoid moiety is estimated to be approximately 23 Å in **1**. The edge-to-edge separation between the π -systems of the carotenoid and tetra-

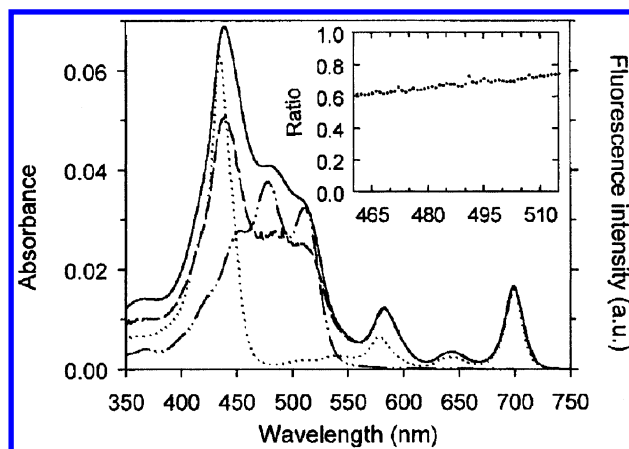


Figure 2. Absorption spectra of dyad **1** (—), purpurin **2** (···), and carotenoid **3** (— · —) in toluene. The corrected fluorescence excitation spectrum of a $\sim 6 \times 10^{-7}$ M solution of **1** in toluene (---), normalized to the absorption spectrum at the purpurin Q_x band (583 nm), is also shown. The fluorescence excitation spectrum was corrected in the range 320–720 nm using a file generated from the absorption and fluorescence excitation spectra of purpurin **2**. The inset shows the ratio of the normalized fluorescence excitation intensity to the absorbance of dyad **1**, after first subtracting the absorbance of **2** from both spectra.

pyrrole is 3.7 Å (this is the distance between carbon (a) of the purpurin isocyclic ring and carbon (d) of the phenyl group of the carotenoid, see structures). On the other hand, the distance from the carbonyl carbon (b) to carbon (d) of the phenyl group of the carotenoid is ~2.5 Å. The macrocycle of **1** deviates from planarity in the region where the chlorin ring is fused to the adjacent five-membered ring, resulting in a dihedral angle of approximately 25° between the planar region of the macrocycle and the plane of the π -system of the carotenoid. The angle between the carotenoid backbone and the Q_y transition of the tetrapyrrole is estimated to be ~50° or ~130° (assuming the Q transitions are aligned along the N–N molecular axes).

Steady-State Absorption Spectra. The absorption spectra of dyad **1**, reference purpurin **2** (normalized to **1** at the Q_y absorption maximum, 699 nm), and model carotenoid **3** (arbitrary scaling) in toluene are shown in Figure 2. The absorption coefficient of the red-most Q-band of the purpurin compounds **1** and **2** is substantially larger than that of simple porphyrins such as *meso*-tetraphenylporphyrin. Dyad **1** has a Soret maximum at 439 nm and Q-bands at 583, 643, and 699 nm. The broad bands at 484 and 515 nm (maxima determined from the analysis of the second derivative spectrum, not shown) correspond to the absorption of the carotenoid.

From Figure 2 it is clear that there is a change in relative intensity and a red shift (5 nm) of the Q_x band (583 nm) in **1** compared to reference purpurin **2**. After subtraction of the underlying carotenoid absorption, the Soret band of dyad **1** was also found to display a small bathochromic shift compared to **2**, in addition to some broadening and a change in relative intensity. Similarly, the carotenoid absorption bands of **1** show red shifts of ~5 nm and a substantial loss of fine structure between 470 and 520 nm relative to model **3**.

Steady-State Fluorescence Studies. In toluene, dyad **1** has purpurin fluorescence emission maxima at 708 and ~ 777 nm and purpurin **2** has maxima at 706 and ~ 770 nm. The emission of **1** and **2** (Figure 3) shows approximate mirror symmetry with their Q_y absorption bands but is broadened slightly. The quantum yield of fluorescence was determined by the comparative method with *meso*-tetraphenylporphyrin as the standard ($\Phi_f = 0.11$).¹⁴ The quantum yield of **1** is 0.10, whereas reference purpurin **2**

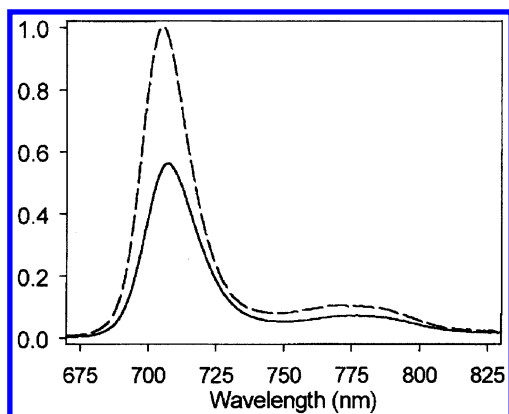


Figure 3. Corrected fluorescence emission spectra of $\sim 3 \times 10^{-6}$ M solutions of dyad **1** (—) and purpurin **2** (---) in toluene. The excitation was at 580 nm.

has a quantum yield of 0.16. The presence of the carotenoid moiety in partial conjugation with the macrocycle in **1** is responsible for the quenching of the tetrapyrrole fluorescence (see fluorescence lifetime data). Similar effects were observed in related compounds.^{15–19}

Fluorescence excitation measurements were performed to measure the efficiency of singlet–singlet energy transfer from the carotenoid to the tetrapyrrole fluorophore. The corrected fluorescence excitation spectrum of dyad **1** in toluene, normalized to the absorption maximum at 583 nm, is presented in Figure 2. Using these normalized spectra, the yield of singlet energy transfer was determined from the ratio of the corrected excitation spectrum to the absorption of **1**, after first subtracting the absorption spectrum of **2**, normalized at 699 nm, from both spectra. The ratio plotted in the range 460–515 nm, where the purpurin moiety has minimal absorption, is shown in the inset of Figure 2. The ratio (average quantum yield of energy transfer) in this range is 0.67 ± 0.04 , although a small increase in the ratio with increasing wavelength is apparent.²⁰

Time-Resolved Fluorescence Studies. The lifetime of the fluorescent S_1 state of the purpurin was determined for **1** and purpurin **2**. A toluene solution of **2** was excited with ~ 9 ps laser pulses at 590 nm, and the fluorescence decay was measured using the time-correlated single photon counting technique. The fluorescence, detected in the 670–770 nm range, decayed monoexponentially with a lifetime of 3.01 ns ($\chi^2 = 1.05$). A similar solution of **1** was excited at 590 nm, and the fluorescence decay was measured at fourteen wavelengths in the 670–800 nm region. To fit the data globally, two exponential components with lifetimes of 1.01 ns (32%) and 1.79 ns (68%) were required ($\chi^2 = 1.08$). Similar observations were obtained with other solvents.²¹

Fluorescence Upconversion Studies. To accurately determine both the decay kinetics of the S_2 state of the carotenoids and the rise kinetics of the purpurin emission, a fluorescence upconversion spectrometer with a ca. 130 fs instrument response function was employed. Excitation in the 480–490 nm region, provided by a frequency-doubled Ti:sapphire laser operated at 82 MHz, was primarily used, ensuring selective excitation of the carotenoids. The S_2 state lifetime of the carotenoid moiety of dyad **1** was measured at emission wavelengths longer than 530 nm and compared to the S_2 state lifetime of the model carotenoid **3**. Fluorescence upconversion decays of **1** and **3** in toluene at 610 nm, along with a Gaussian instrument response function, are shown in Figure 4. The transient emission from carotenoid **3** decays with essentially a single time constant. The average lifetime of the S_2 state, determined from repeated

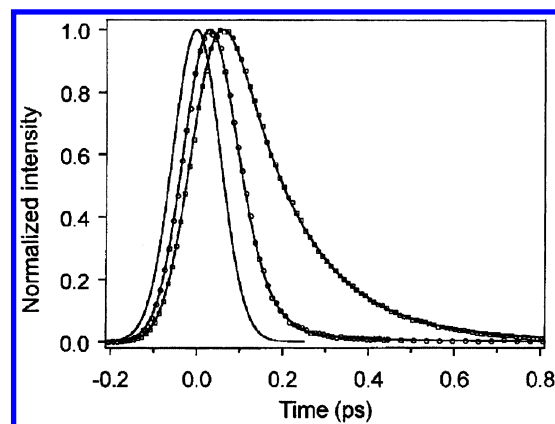


Figure 4. Normalized fluorescence decay kinetics at 610 nm of a $\sim 1 \times 10^{-4}$ M solution of dyad **1** (○) and carotenoid **3** (□) in toluene following excitation with parallel polarization at 481 nm. The lines are fits with decay time constants of 42 fs (98.7% amplitude) and 151 fs (99.1%), the carotenoid S_2 lifetimes of **1** and **3** (at 610 nm), respectively. Also shown is a 130 fs instrument response function.

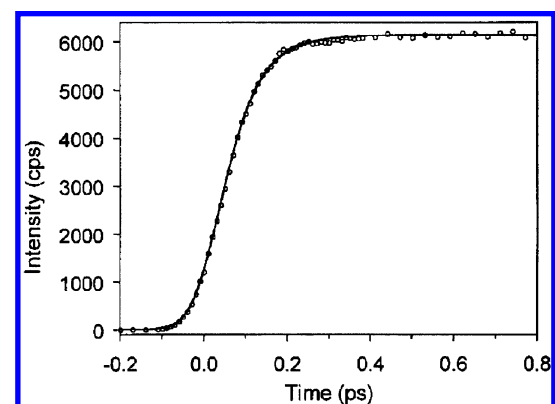


Figure 5. Isotropic formation kinetics of the excited S_1 state of the purpurin moiety of dyad **1** detected by upconversion of the purpurin fluorescence at 699 nm, following excitation at 490 nm with magic angle polarization of a $\sim 1 \times 10^{-4}$ M solution of dyad **1** in toluene.

measurements at five different emission wavelengths, is 150 ± 3 fs (SD of 26). The S_2 lifetime of the carotenoid moiety of **1** is considerably shorter and the average lifetime of the major decay component is 40 ± 3 fs (SD of 20). If this quenching is attributed entirely to singlet–singlet energy transfer from the carotenoid S_2 state to the purpurin moiety, the quantum yield of this process is

$$\Phi_{\text{et}} = 1 - (\tau_{\text{q}}/\tau_{\text{f}}) \quad (3)$$

where τ_{q} and τ_{f} are the S_2 lifetimes of the carotenoid moiety of the dyad and model system, respectively. For dyad **1**, $\Phi_{\text{et}} = 0.73 \pm 0.06$, in reasonable agreement with the steady-state determination.

Direct evidence establishing that energy is transferred from the carotenoid S_2 state was obtained by monitoring the formation of the S_1 excited state of the purpurin moiety of **1** at wavelengths longer than ~ 690 nm. The simplest fluorescence kinetics were observed at 699 nm and the emission measured with the excitation polarization set at the magic angle (54.7° relative to the near-IR laser gating beam used to upconvert the emission) is presented in Figure 5. At this wavelength, the purpurin fluorescence rises with a single time constant of 64 fs and decays only slightly on the 5 ps time range. The absence of any slower rise components at 699 nm is particularly significant and suggests that the S_2 state of the carotenoid functions as the sole

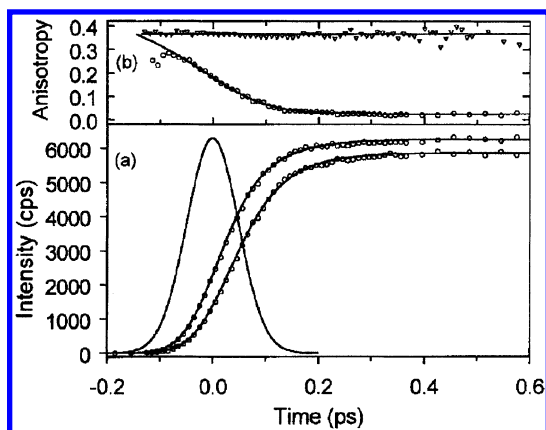


Figure 6. (a) Anisotropic formation kinetics of the excited state (S_1) of the purpurin moiety of dyad **1** detected by upconversion of the purpurin fluorescence at 699 nm, recorded with parallel (top) and perpendicular (bottom) polarized excitation at 490 nm of a $\sim 1 \times 10^{-4}$ M solution of dyad **1** in toluene. (b) Anisotropy calculated from the raw anisotropic kinetics at 603 nm (∇) and 699 nm (\circ). The average anisotropy at 603 nm (0.37) is indicated with a straight line, and the curved line starting at ~ 0.35 and reaching a final value of 0.022 is the anisotropy at 699 nm.

energy donor. Nevertheless, an additional ~ 1.4 ps component with minor amplitude ($\leq 8\%$) is revealed in the isotropic emission kinetics recorded at eight additional wavelengths between 688 and 731 nm. However, because this component is absent at 699 nm, and it appears as a decay (rise) at shorter (longer) wavelengths, it cannot be assigned to a second energy transfer pathway from the carotenoid on the picosecond time scale. Instead, an intramolecular relaxation process in the purpurin singlet manifold is the most likely explanation for the wavelength-dependent behavior of this component (see Supporting Information).²²

Further confirmation of an ultrafast energy transfer pathway from the carotenoid moiety of dyad **1** is provided by time-resolved fluorescence anisotropy measurements made at several wavelengths. The parallel (upper) and perpendicular (lower) polarized emission data points used to calculate the anisotropy at 699 nm are plotted in the bottom panel (a) of Figure 6. Superimposed on these data are fit curves obtained by convoluting a sum of two exponentials (a 64 fs rise and a > 500 ps decay) with the 115 fs response time. The observed anisotropy,

$$R(t) = [I_{\parallel}(t) - I_{\perp}(t)]/[I_{\parallel}(t) + 2I_{\perp}(t)] \quad (4)$$

calculated point-by-point from the experimental data (raw anisotropy) recorded at 699 and 603 nm is shown in the top panel (b). The anisotropy of the carotenoid S_2 state emission at 603 nm is approximately constant, and the average value of 0.37 ± 0.01 is indicated with a straight line. This high anisotropy value is close to the theoretical maximum of 0.4 expected when the absorption and emission transition dipoles of an isolated chromophore are parallel,²⁴ consistent with assignment to the carotenoid S_2 state. In the region of purpurin emission, there is a substantial decay in the anisotropy within the instrument response time. At 699 nm, the raw anisotropy reaches a maximum value of 0.28. However, this occurs on the rising edge of the excitation pulse where low levels of noise result in large errors in the initial value of the anisotropy. Calculating the anisotropy from the fits to the polarized emission data removes errors introduced by the noise and suggests an initial anisotropy value of at least 0.35 (curved line, top panel (b) of Figure 6). This anisotropy curve decays to a minimum value of 0.022 by 0.4 ps and remains constant for a further 4 ps.

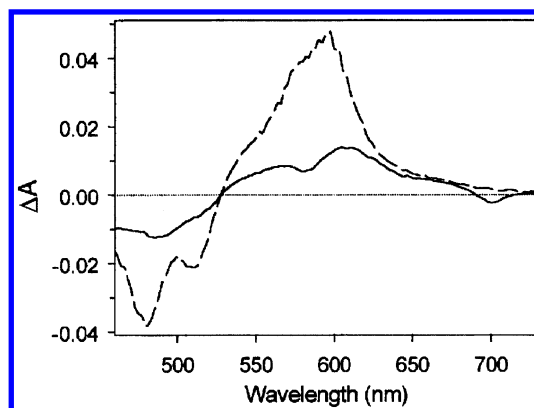


Figure 7. Transient absorption spectra of dyad **1** (—) and carotenoid **3** (---) in toluene at 1.00 ps after excitation at 488 nm with magic angle polarization. The solutions of **1** and **3** were $\sim 5 \times 10^{-5}$ M, and the spectra have been normalized to reflect equal absorbance at the excitation wavelength.

To determine the time constant of the ultrafast anisotropy decay, the response function must be deconvoluted. This was achieved by simultaneous fitting of the isotropic kinetics, calculated from the parallel and perpendicular polarized emission kinetics by eq 5, and the polarization difference eq 6,

$$I_{\text{iso}}(t) = [I_{\parallel}(t) + 2I_{\perp}(t)]/3 \quad (5)$$

$$I_{\parallel}(t) - I_{\perp}(t) = 3I_{\text{iso}}(t) r(t) \quad (6)$$

and by assuming that the decay of the true anisotropy, $r(t)$, is monoexponential. At 699 nm, the depolarization of the emission occurs with a 40 fs time constant from an initial anisotropy of 0.38 to a final value of 0.023.²⁵ Using the relationship,

$$r(t) = (3 \cos^2 \theta - 1)/5 \quad (7)$$

and the final anisotropy values of 0.012–0.033 determined between 688 and 712 nm,²⁵ the angle, θ , between the absorption and emission transition dipoles is calculated to lie in the range 54 – 52° , or its complement, 126 – 128° . These values are close to the 50° or 130° angle between the carotenoid backbone and the Q_y transition of the purpurin that was estimated by molecular modeling methods. Therefore, the observation of a high initial anisotropy of ~ 0.4 is attributed to some overlapping emission from the S_2 state of the carotenoid moiety of **1**, and the ultrafast depolarization is a confirmation of energy transfer to the purpurin.

Time-Resolved Absorption Studies. To determine whether the S_1 singlet excited state of the carotenoid is also involved as a donor of singlet excitation energy to the macrocycle of dyad **1**, transient absorption measurements on the picosecond time scale were made. Figure 7 shows the transient absorption spectra of dyad **1** and carotenoid **3** in toluene obtained 1 ps after an excitation pulse of ~ 100 fs at 488 nm. The spectrum of carotenoid **3** clearly shows the bleaching of the carotenoid bands with a maximum bleach at ~ 480 nm and the broad absorption of the carotenoid excited state ($S_1 \rightarrow S_n$) with a maximum at 598 nm. The transient absorbance spectrum of dyad **1** resembles that of carotenoid **3** superimposed with the bleaching of the purpurin Q-bands at ~ 580 and 700 nm. As a result of efficient energy transfer from the S_2 state, the carotenoid transient absorption amplitude of **1** at 1 ps is significantly smaller than that of carotenoid **3**. The contribution from the purpurin can be removed by subtracting the transient absorption spectrum at 100 ps (not shown) from the 1 ps spectrum. The resulting excited-

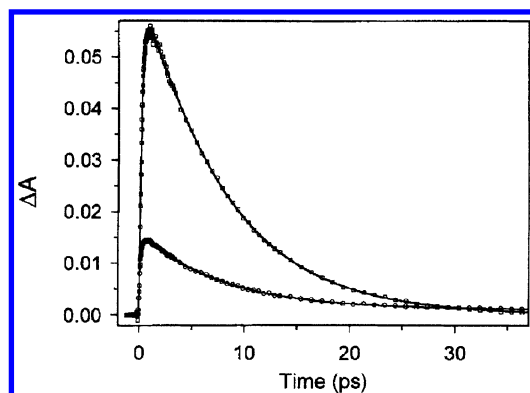


Figure 8. Transient absorption of dyad **1** (○) and carotenoid **3** (□) probed at 598 nm following excitation of $\sim 5 \times 10^{-5}$ M toluene solutions having the same absorbance at 488 nm. The fits (convoluted with a 140 fs response function) are 42 fs (−0.55), 0.24 ps (−0.45), 7.67 ps (0.93), and >1.0 ns (0.07) for **1** and 0.20 ps (−0.88), 1.4 ps (−0.12), and 7.76 ps (1.00) for **3**. The major decay component of these transients corresponds to the lifetime of the carotenoid S_1 state; ~ 7.7 ps in both cases. The values in parentheses indicate relative amplitudes.

state absorption of the carotenoid moiety of dyad **1** is broader than that of carotenoid **3**, and the maximum is shifted to ~ 604 nm. In the region of carotenoid bleaching, only one clear band at ~ 484 nm is observed. The loss of fine structure and the red shifts compared to carotenoid **3** are in agreement with the steady-state absorption spectra of these compounds (vide supra).

Figure 8 presents the transient absorption decay kinetics probed at 598 nm, close to the peak of the carotenoid $S_1 \rightarrow S_n$ excited-state absorption, for carotenoid **3** and dyad **1**. The amplitude of the carotenoid S_1 absorption of **1** at 598 nm is only 26% of that of **3**. The lifetime of the carotenoid S_1 state determined from the decay of these transients is 7.8 ± 0.1 ps for reference carotenoid **3** and 7.7 ± 0.1 ps for dyad **1**. These S_1 lifetimes are the same, within experimental error, indicating that energy transfer from the S_1 state of the carotenoid to the purpurin is negligible.²⁶

Transient absorption spectra at several time delays were also recorded for **1** in 2-methyltetrahydrofuran. Figure 9a shows the transient absorption spectra of dyad **1** obtained at 0 ps, 50 ps, and 4 ns probe delay after a ~ 100 fs pulse of 510 nm light. At this wavelength, the carotenoid moiety absorbs 95% of the excitation light (see Figure 2). The spectrum obtained at zero probe delay is essentially the same as the 1 ps spectrum of Figure 7 in the same wavelength range. At 50 ps, the main feature is the bleaching of the purpurin Q_x band at 578 nm. The time constant for the recovery of this bleach is 1.4 ns, matching the average S_1 lifetime of the purpurin moiety of **1** determined by time-correlated single photon counting in the same solvent.²¹ At 4 ns, the dominant feature of the transient spectrum is the strong absorption at 540 nm, which is assigned to the carotenoid triplet species.²⁷ The rise of this signal is illustrated in Figure 9b, and it also occurs with the same time constant (1.40 ns) as the decay of the purpurin first excited singlet state. Nanosecond transient absorption measurements indicate that the carotenoid triplet state decays with a time constant of 5 μ s in argon-saturated toluene.

Discussion

Absorption Spectrum Perturbation. The absorption spectrum of dyad **1** is perturbed compared to a linear combination of the spectra of models of the macrocycle **2** and carotenoid **3**.

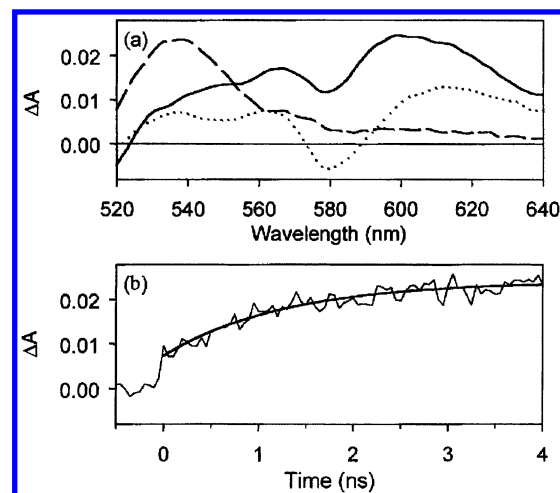


Figure 9. (a) Transient absorption spectra at several time delays for a $\sim 10^{-5}$ M solution of dyad **1** in 2-methyltetrahydrofuran. Probe delay: 0 ps (—), 50 ps (···), and 4 ns (---) after a ~ 100 fs laser pulse at 510 nm. (b) Formation kinetics of the carotenoid triplet state signal at 540 nm. The solid line is a single-exponential fit to the data with a 1.4 ns time constant.

The perturbation is most obvious for the purpurin absorption bands lying to either side of the carotenoid absorption maxima. The substantial relative change in intensity of the Q_x absorption band at 583 nm and the Soret is of particular note. In addition, there are bathochromic shifts of all the bands lying between 400 and 600 nm compared to the model systems **2** and **3**. Similar perturbations have also been observed in dyads comprising a carotenoid directly linked by an aromatic group to the meso position of a porphyrin.¹⁷ The origin of the perturbation of the spectrum of **1** is most likely interchromophore interactions arising from partial conjugation via the amide linkage. However, it is important to note that the transient absorption and emission spectra of dyad **1** remain similar to those of the model systems, indicating that the coupling is not so strong that the spectral identity of the excited singlet states of the individual chromophores is lost.

Quenching Pathways of the S_1 State of the Cyclic Tetrapyrrole. The steady-state fluorescence emission spectra of **1** and **2** are similar in shape and are typical of porphyrin-like macrocycles. Dyad **1** does, however, exhibit a Stokes shift (9 nm) that is 2 nm larger than that of model purpurin **2**. The fluorescence quenching that is observed for **1** compared to **2** has been seen in other covalently linked dyads of this general type.^{15–19} The fluorescence decay of **1** is biexponential in all the solvents tested, and the lifetimes of the S_1 state of the purpurin moiety decrease with increasing solvent polarity. This solvent sensitivity suggests that one possible mechanism for the quenching is electron transfer from the carotenoid to the purpurin S_1 state,¹⁵ resulting in the charge separated state $C^{+}P^{-}$, as has been observed in a related system.¹⁶ However, other mechanisms, including singlet energy transfer from the macrocycle to the S_1 state of the carotenoid, have also been considered as plausible explanations for the observed quenching.³ Support for this quenching mechanism comes from more recent studies on carotenoporphyrin dyads that show substantial quenching ($> 85\%$) of the S_1 state of the porphyrin, independent of the solvent polarity.^{18,19} The presence of two isomeric populations, possibly due to restricted rotation about the linkage bonds, differences in the locations of the central hydrogen atoms on the macrocycle, or isomerism involving the two chiral centers, is a possible explanation for the biexponential fluorescence decay of **1**.

Singlet–Singlet Energy Transfer from the Carotenoid.

The appreciable signal intensity in the 460–540 nm spectral region of the corrected fluorescence excitation spectrum (Figure 2) indicates that light energy harvested by the carotenoid of dyad **1** is efficiently transferred to the purpurin. The quantum yield of this singlet–singlet intramolecular energy transfer in dyad **1**, determined from the ratio between the corrected excitation and absorption spectra, is 0.67 ± 0.04 . The yield is remarkably high compared to other dyads consisting of carotenoids covalently linked to porphyrin-type macrocycles.^{15–17,27,28} Moreover, the time-resolved fluorescence and absorption measurements on **1** and model carotenoid **3** reveal that this efficient energy transfer is achieved exclusively from the S_2 state of the carotenoid. The kinetic evidence establishing that the carotenoid S_2 state is the sole energy donor is as follows:

- The S_2 lifetime of the carotenoid, determined by fluorescence upconversion, is reduced from 150 to 40 fs (see Figure 4) when the carotenoid is covalently linked to the purpurin. In contrast, the lifetimes of the carotenoid S_1 states of dyad **1** and model **3** probed at 598 nm, which is close to the $S_1 \rightarrow S_n$ transient absorption maximum (see Figure 8), are the same, within experimental error.

- The observation of ultrafast isotropic purpurin rise kinetics, which are single exponential at 699 nm (64 fs) and as short as 44 fs at 688 and 712 nm (Supporting Information), rules out the involvement of any other carotenoid singlet state.²⁹ In addition, these results verify that at least some of the S_2 state quenching is the result of energy transfer. The difference between the carotenoid S_2 state decay of 40 fs and the tetrapyrrole S_1 state rise of 64 fs at 699 nm is, therefore, attributed to a delay associated with vibronic relaxation in the tetrapyrrole (see Supporting Information).

- Quantitatively, quenching of the carotenoid S_2 state from 150 to 40 fs yields an energy transfer efficiency of $73 \pm 6\%$, in satisfactory agreement with that measured by steady-state fluorescence excitation spectroscopy ($67 \pm 4\%$). Furthermore, the formation yield of the S_1 state of the carotenoid moiety of dyad **1** is reduced to $\sim 26\%$ of that of model **3** (see Figures 7 and 8).

- The ultrafast anisotropy decay from 0.38 to 0.023 with a 40 fs time constant at 699 nm (see Figure 6) indicates a change in angle of 127° between the absorption and emission transition dipoles, which is in excellent agreement with that estimated by molecular modeling methods.

To calculate accurate energy transfer efficiencies from the S_1 and S_2 states of the carotenoid moiety of dyad **1**, it is essential to know the excited-state lifetimes in the absence of energy transfer. Here we have assumed that carotenoid **3** is a suitable model system and the reduction in the S_2 lifetime is entirely the result of energy transfer quenching. Carotenoid **3** is not a perfect model, as coupling of the carotenoid to the purpurin results in a ~ 5 nm red shift of both the $S_0 \rightarrow S_2$ and $S_1 \rightarrow S_n$ absorption maxima. However, estimates of the effects of such a shift on carotenoid singlet lifetimes, based on a variety of model carotenoids, including *all-trans*- β -carotene,³² γ -carotene, and lycopene in toluene, indicate that the effect is negligible.

The lack of energy transfer from the carotenoid S_1 state,³³ as indicated by the similar lifetimes found for the S_1 states of **1** and **3**, can be rationalized on energetic grounds. The energy of the forbidden S_1 state of the carotenoid, ΔE_{10} , of dyad **1** is uncertain, but it can be estimated using the energy gap law³⁴ with the parameters reported for *all-trans*- β -carotene and some shorter chain analogues.^{35,36}

$$\ln k_1 = 35.9 - (7.39 \times 10^{-4})\Delta E_{10} \quad (8)$$

The energy of the S_1 state of model carotenoid **3** calculated from the experimentally determined deactivation rate of the S_1 state, k_1 , is $13\,960\text{ cm}^{-1}$ (716 nm). An alternative approach to estimating the S_1 energy of **3** is to assume that the S_1 and S_2 energies decrease in parallel and that the S_1 state, therefore, lies at $\sim 650\text{ cm}^{-1}$ below that of *all-trans*- β -carotene ($14\,200 \pm 500\text{ cm}^{-1}$ in carbon disulfide³⁶ or $14\,500 \pm 50\text{ cm}^{-1}$ in *n*-hexane at 170 K).³⁷ This approach yields an upper limit for the S_1 energy of **3** of $13\,850\text{ cm}^{-1}$ (722 nm). Thus, both approaches indicate that the S_1 state of the carotenoid lies below that of the purpurin moiety of **1**, which has an S_1 energy of $14\,215\text{ cm}^{-1}$ (703 nm), taken as the midpoint between the Q_y (0,0) absorption and emission maxima. Rapid energy transfer from the carotenoid S_1 to the purpurin is therefore precluded on thermodynamic grounds.

It is interesting to compare the kinetics observed for dyad **1** with those observed in some natural systems. The rate of energy transfer from the carotenoid S_2 state in the model system ($1.8 \times 10^{13}\text{ s}^{-1}$) is more than 3 times faster than that observed in the peripheral light-harvesting (LH2) complex of *Rhodospseudomonas acidophila* and of the same order as that observed in the LHCII complexes of higher plants. In the case of *R. acidophila*, a rate constant of $5.4 \times 10^{12}\text{ s}^{-1}$ has been measured for energy transfer from the S_2 state of the carotenoid (rhodopin glucoside) to the B850 bacteriochlorophylls that are in close proximity.⁹ The carotenoid lies across the face of the B850 bacteriochlorophylls and is in van der Waals contact ($\sim 3.6\text{ \AA}$) with the α -B850.³⁸ On the other hand, the rate constant for energy transfer from rhodopin glucoside to the B800 bacteriochlorophyll in the same complex is only slightly slower at $3.6 \times 10^{12}\text{ s}^{-1}$.⁹ These chromophores are also in close proximity, but the geometry is very different; the carotenoid is approximately perpendicular to the plane of the B800 bacteriochlorophyll and in van der Waals contact ($\sim 3.4\text{ \AA}$) with its edge.³⁸

The S_2 state lifetime of the carotenoid in both the model system and the natural LH2 system in the absence of energy transfer are of the same order (150 fs and ~ 120 fs, respectively).⁹ The 3-fold larger rate constant for energy transfer in the dyad results in improved energy transfer efficiency: $\sim 70\%$ in the model system, in contrast to $\sim 30\%$ in *R. acidophila* (from the carotenoid to B850). It should also be pointed out that the carotenoid S_2 state is the dominant donor in the LH2 of *R. acidophila*, and an increase in light-harvesting efficiency is achieved by having more than one energy acceptor. Furthermore, some energy transfer occurs from the S_1 state, indicating that this pathway is energetically possible, in contrast to the model system, where it is precluded by energetics.

Although high-resolution structures are not yet available,³⁹ it is worth mentioning the similarities between the dynamics of dyad **1** and the chlorophyll *a/b* light-harvesting complex LHCII of photosystem II, the most abundant antenna system of higher plants. In LHCII, the efficiency of excitation energy transfer from the S_2 state of the xanthophyll carotenoids to chlorophyll has been reported to be 50–80%.^{40–43} The lifetime of the S_2 state of the xanthophylls in LHCII trimers is only ~ 26 fs and, in the absence of energy transfer, the intrinsic S_2 lifetime of the xanthophylls is ~ 120 fs, as measured by fluorescence upconversion.⁴³ From these S_2 lifetimes, an energy transfer efficiency of 78% and a rate of $3.0 \times 10^{13}\text{ s}^{-1}$ are obtained, making this energy transfer process one of the fastest occurring in nature.⁴⁴

Mechanistic Considerations. Energy transfer from carotenoid antenna pigments to chlorophylls can be brought about by a variety of interactions. Within the framework of the Fermi Golden Rule, these energy transfer processes are controlled by the product of a spectral overlap integral and an electronic coupling term. The spectral overlap integral between the S_2 emission of the carotenoid in **1**, approximated as the emission of *all-trans*- β -carotene in toluene shifted 650 cm^{-1} lower in energy and the Q_x absorption of purpurin **3** is calculated to be $2.6 \times 10^{-4}\text{ cm}$ (between 506 and 616 nm), which is similar to the S_2 - Q_x overlap value reported for LH2.⁸ Turning to the electronic coupling term, a value of 130 cm^{-1} for the dipole–dipole coupling between the S_2 state of the carotenoids and the Q_x transition of bacteriochlorophyll *a* in LH2 has been calculated for a center-to-center distance of 14.2 \AA .^{8,45} Higher values (up to 500 cm^{-1}) were calculated for the coupling of the lutein S_2 state with the Q_x and Q_y transitions of chlorophyll *a* in LHCII at distances as short as 7.6 \AA .⁴¹ Interestingly, the electronic couplings estimated from the experimental rates and the spectral overlap integrals for dyad **1** is 240 cm^{-1} ; a value comparable to those calculated for the natural systems.^{8,41}

As the chromophores are brought closer together, higher order electrostatic terms begin to make significant contributions to the electronic coupling matrix elements. The inclusion of these terms can relax the need for strong, dipole-allowed transitions and relatively long-lived states in the donor and can account for the carotenoid S_1 and S_2 levels acting as donor states.⁴⁶ In the most recent and complete description of the electronic coupling, the change in the electron density accompanying the electronic transition is calculated for each atom (point dipoles) of the two chromophores. The interactions between the point dipoles are then summed throughout the volume of the donor and acceptor (transition density calculations).^{8,47} Thus, more exact Coulombic coupling terms can be determined, even when the two chromophores are in close proximity and local interactions make the dominant contributions to the coupling. Coupling terms sufficiently large to result in subpicosecond rates are obtained for LH2 but require the short distances associated with van der Waals contact.^{8,47} In model system **1**, the covalent bond linking the carotenoid to the tetrapyrrole fixes the distance between the closest π -orbitals of the two chromophores at approximately the sum of their van der Waals radii. ($\sim 3.7\text{ \AA}$ distance from (a) to (d) or $\sim 2.5\text{ \AA}$ distance from (b) to (d), see structures).

Once the π -systems of the chromophores are brought into van der Waals contact, the contribution of Dexter electron-exchange and other short-range interactions to the electronic coupling term should also be considered.^{10,48,49} However, calculations suggest that the Dexter electron-exchange term is insignificant compared to Coulombic coupling of the singlet excited states of the carotenoids and bacteriochlorophylls.^{46,47} Nevertheless, the chromophores of the model system are covalently linked and it is expected that the bridge atoms will play an important role in mediating the electron exchanges. The Dexter mechanism requires donor–acceptor orbital overlap but does not depend on monopole, dipole, or multipole strengths and is the accepted mechanism for triplet–triplet energy transfer. How fast can Dexter-mediated energy transfer be, and to what extent do electron exchange-based electronic coupling matrix elements contribute to singlet energy transfer in these systems? In dyad **1** and several other carotenoid-containing multichromophoric molecules energy transfer from the triplet tetrapyrrole to populate the carotenoid triplet state (triplet–triplet energy transfer) is immeasurably faster than intersystem crossing.¹⁵ This

is illustrated in Figure 9a, which presents the spectrum with a maximum at 540 nm characteristic of the carotenoid $T_1 \rightarrow T_n$ excited-state absorption. This spectrum is taken 4 ns following excitation of the porphyrin moiety of dyad **1** in 2-methyltetrahydrofuran solution with a $\sim 100\text{ fs}$ pulse of 510 nm light. The rise of the carotenoid triplet species (measured at 537 nm) is presented in Figure 9b. The 1.40 ns rise time is identical to the 1.4 ns weighed average fluorescence lifetime of **1** under the same conditions.²¹ The agreement between the rise time of the triplet energy acceptor and the singlet lifetime of the triplet energy donor indicates that intersystem crossing in the donor is the rate-limiting step in the flow of energy from the singlet of the donor to the triplet of the acceptor, and the true rise time of the triplet carotenoid could be much faster than intersystem crossing in the tetrapyrrole.⁵⁰ However, the extent to which electron exchange-based mechanisms contribute to singlet energy transfer on the $<100\text{-fs}$ time scale in these systems is not obvious and awaits detailed quantum chemical calculations.

The role of a Dexter-based mechanism has been addressed experimentally in one study of three isomeric carotenoporphyrins in which the singlet–singlet energy transfer efficiency (albeit with much lower efficiency and therefore slower rates than observed in dyad **1**) and triplet–triplet energy transfer rates were found to depend in the same way on the electronic structure of the interchromophore linkage group.¹⁵ Because the triplet energy transfer process is necessarily mediated by the Dexter mechanism, a simple interpretation is that in these dyads, the slower and less efficient singlet energy transfer is at least partially mediated by electron exchange terms. However, in dyad **1** of the present study, the observation that the covalently linked model system achieves a rate similar to those found in the natural protein complexes for similar edge-to-edge distances between the π -systems provides no indication that the covalent bonds introduce any specific term in the electronic coupling that is important in the ultrafast energy transfer process.

Conclusions

The steady-state fluorescence excitation and ultrafast fluorescence upconversion measurements on synthetic dyad **1** reported in this paper demonstrate efficient singlet–singlet energy transfer from the carotenoid pigment to the cyclic tetrapyrrole. Fluorescence upconversion measurements were used to determine the lifetime of the short-lived S_2 state of a model for the carotenoid moiety of **1** in solution and of the carotenoid moiety of **1** covalently linked to the energy acceptor. These data together with pump–probe absorption results clearly indicate that the S_2 state of the carotenoid transfers excitation energy to the singlet manifold of the cyclic tetrapyrrole with a rate constant of $1.8 \times 10^{13}\text{ s}^{-1}$. The carotenoid S_1 state does not transfer energy to the cyclic tetrapyrrole in dyad **1**.

Regardless of the mechanism, the structural criterion for significant singlet–singlet energy transfer in every carotenoid-containing system examined to date, either a naturally occurring pigment protein complex or a synthetic carotenotetrapyrrole, is that the chromophores be in van der Waals contact or have π -orbital contact provided by the interchromophore linkage.

The simple dyad described herein mimics the ultrafast energy transfer kinetics found in naturally occurring pigment protein complexes and is thus able to reproduce the high electronic coupling needed for efficient energy transfer from an extremely short-lived energy donor state. Although not discussed in this work, the attached carotenoid in dyad **1** provides photoprotection from singlet oxygen sensitization, mimicking that found in the LH2 and LHCII complexes. This molecular architecture will

be used in the design of highly efficient artificial light-harvesting systems with increased optical absorbance at wavelengths of maximal solar irradiance.

Experimental Section

Instrumental Techniques. The ^1H NMR spectra were recorded on Varian Unity spectrometers at 300 or 500 MHz. Unless otherwise specified, samples were dissolved in deuteriochloroform with tetramethylsilane as an internal reference. Mass spectra were obtained on a Kratos MS 50 mass spectrometer operating at 8 eV in FAB mode (high resolution) or with a matrix-assisted time-of-flight spectrometer (matrix used: sulfur, low resolution). Measured mass/charge ratios (m/z) and ^1H NMR data are listed for each compound. Ultraviolet–visible absorption spectra were measured on Beckman DU-70 or Shimadzu UV2100U UV–vis spectrometers, and corrected fluorescence excitation and emission spectra were obtained using a SPEX Fluorolog 112 and optically dilute samples ($A < 0.07$). The excitation spectrum of the reference tetrapyrrole **2** was recorded under identical conditions and used to generate a correction file by assuming that the absorption and fluorescence excitation spectra were identical. The bandwidth of the excitation and emission monochromators was 1.8 and 3.6 nm, respectively. Fluorescence quantum yields were determined by comparison to a standard, *meso*-tetraphenylporphyrin (Aldrich) in air-saturated benzene ($\Phi_f = 0.11$).¹⁴ Standard corrections were made for the wavelength response and number of absorbed photons at the excitation wavelength (580 and 640 nm).

Fluorescence decays on the pico/nanosecond time scale were performed on $\sim 1 \times 10^{-5}$ M solutions by the time-correlated single photon counting method. The excitation source was a frequency-doubled Nd:YAG laser (Coherent Antares 76s) routed through a variable beam splitter to pump a dye laser cavity-dumped at 3.6 MHz.⁵¹ The instrument response function was 35 ps, as measured at the excitation wavelength for each decay experiment with Ludox AS-40. The reported fluorescence lifetimes were determined by global analysis and the χ^2 was lower than 1.1 in each case.

Fluorescence decays on the femto/picosecond time scale were recorded using the fluorescence upconversion technique and a spectrometer that has been modified to give better time response than previously described.³² Excitation light centered in the 481–490 nm region with a 82 MHz repetition rate was obtained by frequency doubling the ca. 70 fs near-infrared pulses produced by a mode-locked Ti:sapphire laser (Spectra Physics, Tsunami) pumped by an argon ion laser. The samples were held in a rotating cell with a 0.5 mm path length, and the energies of the excitation pulses were < 0.25 nJ. Fluorescence decays were recorded at more than twelve wavelengths in the range 533–731 nm using parallel (in the carotenoid S_2 emission region) or magic angle polarization (in the region of the tetrapyrrole emission). In addition, the time dependence of the anisotropy was also studied, by setting the polarization of the excitation beam parallel or perpendicular to the gating beam with a Berek compensator (New Focus). Fluorescence transients were fit to a sum of at least two exponential decays with a floating background and were convoluted with a Gaussian response function, using the SPECTRA program.

Transient absorption measurements on the femto/picosecond time scale were made using the pump–probe technique with a system described previously.⁹ The fourth harmonic of the idler output produced by an optical parametric amplifier (Spectra Physics, OPA-800) operating at 5 kHz was used to produce excitation pulses centered in the region 483–490 nm. Following

compression to < 120 fs by double passing through a SF14 prism pair, the pump beam had a pulse energy of < 40 nJ and spot size of ~ 0.4 mm at the sample, which was held in a static 1 mm path length cuvette. A white light continuum beam was split into two and used as the probe and reference beams, which were spectrally resolved with a monochromator (Yobin Yvon/Horiba, H10 or TRIAX 190) and monitored with silicon photodiodes after the sample. Transient absorption spectra were recorded between 470 and 740 nm with a 2 nm step size and a bandwidth of 3.6 nm. The chirp of the white light was corrected during the scan by active delay line compensation at each wavelength. The chirp correction file was obtained by recording the maximum of the two-photon absorption signal of diphenylhexatriene in toluene at twelve wavelengths in the range 460–840 nm. Kinetics were recorded with variable delay line step sizes with the polarization of the pump beam set at the magic angle with a Berek compensator and the probe beams passed through a cube polarizer after the sample.

Transient absorption measurements on the pico/nanosecond time scale were made using the pump–probe technique with an instrument previously described.⁵² The signal output produced by an optical parametric amplifier (Clark-MXR, IR-OPA) operating at 1 kHz was mixed with the 790 nm pump beam from the Ti:sapphire regenerative amplifier to produce ~ 150 fs excitation pulses at 510 nm. The pump beam was polarized at the magic angle and the energy and spot size at the sample were 2–5 μJ and 0.5–1 mm, respectively. The samples were held in a 2 mm path length cuvette and were circulated by magnetic stirring. Probe and reference beams were produced by white light continuum generation and were focused onto two separated optical fiber bundles coupled to a spectrograph (Acton Research, SP275). The spectra were acquired with a dual diode array detector (Princeton Instruments, DPDA-1024) and the white light dispersion correction was obtained from the birefringent response of carbon disulfide.

The solvents used for the spectroscopic work were toluene (99+%), 2-methyltetrahydrofuran (99.8+%), and dichloromethane (99.5+%) from Merck and benzonitrile (99.9%, HPLC grade) from Aldrich. The solvents were purified by column chromatography with neutral activated Al_2O_3 (Merck, type I) or by distillation. All measurements were made in air-saturated solvents at room temperature, except as noted for the data presented in Figure 9.

Synthesis. Carotenoid **3** (7'-apo-7'-(4-acetamidophenyl)- β -carotene) was prepared by a Wittig type reaction of 8'-apo- β -caroten-8'-al with 4-(*N*-acetylamino)benzyltriphenylphosphonium bromide according to literature methods.¹³ The purpurin ester **2** was prepared by previously published procedures.^{11,12}

Carotenopurpurin 1. To a 500 mL round-bottomed flask equipped with a stirring bar was added 300 mg (0.404 mmol) of **2**, 200 mL of THF, and 50 mL of methanol. Once all the solid had dissolved, 8 mL of 10% aqueous KOH was added dropwise. The solution was warmed to 35 $^\circ\text{C}$ and kept under a N_2 atmosphere for 7 days. After this time, TLC indicated that all the ester had been converted to the corresponding acid. The reaction mixture was poured into a mixture of dichloromethane/10% methanol and washed once with diluted aqueous citric acid and three times with water. Distillation of the organic phase solvents at reduced pressure yielded the purpurin acid (281 mg, 95% yield), which was used in the next step without further purification.

The purpurin acid (250 mg, 0.343 mmol), 20 mL of dichloromethane, and 53 μL (0.480 mmol) of *N*-methylmorpholine

were placed in a 100 mL round-bottomed flask. The solution was cooled to 0 °C before 73 mg (0.412 mmol) of 2-chloro-4,6-dimethoxy-1,3,5-triazine was added to the flask. The solution was stirred at 0 °C under a N₂ atmosphere for 15 min and then at room temperature for another 6 h. At that time, TLC indicated that practically all the purpurin acid was converted to the triazine intermediate. Another portion of *N*-methylmorpholine (53 mL, 0.480 mmol), 190 mg (0.377 mmol) of the aminocarotenoid,¹³ and 84 mg (0.686 mmol) of 4-(dimethylamino)pyridine (DMAP) were added. The mixture was kept well stirred under a N₂ atmosphere for 6 days. TLC indicated the presence of a major product, and the reaction was stopped. The reaction mixture was diluted with dichloromethane and extracted first with diluted aqueous citric acid and then with aqueous NaHCO₃. Residual water was removed with anhydrous Na₂SO₄ and the solvent was evaporated to give a dark brown solid. This material was chromatographed on silica gel (flash column, dichloromethane/2–2.5% acetone) and then recrystallized from dichloromethane/methanol to yield 305 mg (73% yield) of pure carotenopurpurin **1**. ¹H NMR (500 MHz, CDCl₃), δ (ppm): –0.28 (3H, t, Pur 24-CH₃), –0.12 (1H, brs, –NH), 0.78 (1H, brs, –NH), 1.03 (6H, s, Car 16,17-CH₃), 1.47–1.68 (17H, m, Car 2,3-CH₂, Pur 3,9,13-CH₂CH₃, Pur 23-CH, Pur 25-CH₃), 1.72 (3H, s, Car 18-CH₃), 1.98–2.02 (9H, m, Car 19,20,20'-CH₃), 2.14 (3H, s, Car 19'-CH₃), 2.26 (6H, s, 2 × Pur-CH₃), 2.58 (1H, m, Pur 23-CH), 2.59 (3H, s, Pur-CH₃), 2.66 (3H, s, Pur-CH₃), 3.58–3.81 (6H, m, Pur 3,9,13-CH₂CH₃), 4.90 (1H, q, *J* = 5.1 Hz Pur 18-H), 6.11–6.91 (14H, m, Car =CH–), 7.08 (1H, d, *J* = 5.4 Hz, Pur-Ar), 7.25 (1H, d, Pur-Ar), 7.42–7.53 (5H, m, Pur-Ar, Car 1',5'-Ar), 7.59 (1H, d, *J* = 5.7 Hz, Pur-Ar), 7.71 (2H, d, *J* = 6.0 Hz, Car 2',4'-Ar), 7.87 (1H, s, –NH), 7.96 (1H, d, *J* = 5.7 Hz, Pur-Ar), 8.13 (1H, d, *J* = 5.4 Hz, Pur-Ar), 9.21 (1H, s, Pur 21-H), 9.49 (1H, Pur 11-H *meso*). HRFAB-MS *m/z* calcd for C₈₆H₉₇N₅O: 1215.7693. Found: 1216.7786 (*M* + 1)⁺. UV/vis (CH₂Cl₂): 299, 440, 480, 508, 534, 584, 644, and 700 nm.

Acknowledgment. This paper is dedicated to Professor T. George Truscott on the occasion of his retirement from Keele University, U.K.. This work was supported by the Swedish Natural Science Research Council (NFR), the Kempe Foundation, the U.S. Department of Energy (DE-FG03-93ER14404) and the NSF (INT-9600282). We thank Roche for the generous gift of carotenoid samples. This is publication 509 from the ASU Center for the Study of Early Events in Photosynthesis. We thank the Nebraska Center for Mass Spectrometry for FAB high resolution mass spectrometry experiments.

Supporting Information Available: Formation kinetics of the excited S₁ state of the tetrapyrrole of **1** detected by upconversion of the tetrapyrrole fluorescence at different wavelengths. This material is available free of charge via the Internet at <http://pubs.acs.org>.

References and Notes

- (1) Siefertman-Harms, D. *Physiol. Plant.* **1987**, *69*, 561–568.
- (2) Koyama, Y.; Kuki, M.; Andersson, P. O.; Gillbro, T. *Photochem. Photobiol.* **1996**, *63*, 243–256.
- (3) Frank, H. A.; Cogdell, R. J. *Photochem. Photobiol.* **1996**, *63*, 257–264.
- (4) Ricci, M.; Bradforth, S. E.; Jimenez, R.; Fleming, G. R. *Chem. Phys. Lett.* **1996**, *259*, 381–390.
- (5) Trautman, J. K.; Shreve, A. P.; Owens, T. G.; Albrecht, A. C. *Chem. Phys. Lett.* **1990**, *166*, 369–374.
- (6) Trautman, J. K.; Shreve, A. P.; Violette, C. A.; Frank, H. A.; Owens, T. G.; Albrecht, A. C. *Proc. Natl. Acad. Sci. U.S.A.* **1990**, *87*, 215–219.
- (7) Andersson, P. O.; Cogdell, R. J.; Gillbro, T. *Chem. Phys.* **1996**, *210*, 195–217.
- (8) Krueger, B. P.; Scholes, G. D.; Jimenez, R.; Fleming, G. R. *J. Phys. Chem. B* **1998**, *102*, 2284–2292.
- (9) Macpherson, A. N.; Arellano, J. B.; Fraser, N. J.; Cogdell, R. J.; Gillbro, T. *Biophys. J.* **2001**, *80*, 923–930.
- (10) Scholes, G. D.; Harcourt, R. D.; Fleming, G. R. *J. Phys. Chem. B* **1997**, *101*, 7302–7312.
- (11) Gunter M. J.; Robinson B. C. *Aust. J. Chem.* **1990**, *43*, 1839–1860.
- (12) Forsyth T. P.; Nurco D. J.; Pandey R. K.; Smith, K. M. *Tetrahedron Lett.* **1995**, *36*, 9093–9096.
- (13) Gust, D.; Moore T. A.; Moore A. L.; Liddell P. A. *Methods Enzymol.* **1992**, *213*, 87–100.
- (14) Seybold, P. G.; Gouterman, M. *J. Mol. Spectrosc.* **1969**, *31*, 1–13.
- (15) Gust, D.; Moore, T. A.; Moore, A. L.; Devadoss, C.; Liddell, P. A.; Hermant, R.; Nieman, R. A.; Demanche, L. J.; DeGraziano, J. M.; Gouni, I. *J. Am. Chem. Soc.* **1992**, *114*, 3590–3603.
- (16) Hermant, R. M.; Liddell, P. A.; Lin, S.; Alden, R. G.; Kang, H. K.; Moore, A. L.; Moore, T. A.; Gust, D. *J. Am. Chem. Soc.* **1993**, *115*, 2080–2081.
- (17) Osuka, A.; Yamada, H.; Maruyama, K.; Mataga, N.; Asahi, T.; Ohkouchi, M.; Okada, T.; Yamazaki, I.; Nishimura, Y. *J. Am. Chem. Soc.* **1993**, *115*, 9439–9452.
- (18) Cardoso, S. L.; Nicodem, D. E.; Moore, T. A.; Moore, A. L.; Gust, D. *J. Braz. Chem. Soc.* **1996**, *7*, 19–29.
- (19) Shinoda, S.; Tsukube, H.; Nishimura, Y.; Yamazaki, I.; Osuka, A. *J. Org. Chem.* **1999**, *64*, 3757–3762.
- (20) This wavelength dependence (the ratio reaches 0.95 at 570 nm) is probably the result of underestimating the underlying contribution of the purpurin absorption in the Q_x region, which is much weaker for purpurin **2** compared to dyad **1**.
- (21) Lifetimes of the S₁ state of the purpurin moiety of **1**: 1.07 ns (89%) and 2.53 ns (11%) in THF ($\chi^2 = 1.02$); 0.63 ns (76%) and 1.20 ns (22%) in dichloromethane ($\chi^2 = 1.11$); 1.7 ns (60%) and 1.07 ns (40%) in 2-methyltetrahydrofuran ($\chi^2 = 1.09$); 0.30 ns (87%) and 0.66 ns (11%) in benzonitrile ($\chi^2 = 1.08$).
- (22) The wavelength-dependent behavior of the ~1.4 ps component has only a small effect on the shape of the time-dependent fluorescence spectra, reconstructed after normalization of the isotropic kinetics to the steady-state fluorescence spectrum (Figure 3). There is no shift in the emission maximum between 0.3 and 4.3 ps and only a small (~1 nm) decrease in the bandwidth. We assign the 1.4 ps time constant to cooling of the vibrationally hot purpurin molecules, which are produced following ultrafast (<100 fs) relaxation from higher vibronic or electronic levels.²³
- (23) Elsaesser, T.; Kaiser, W. *Annu. Rev. Phys. Chem.* **1991**, *42*, 83–107.
- (24) Cantor, C. R.; Schimmel, P. R. *Biophysical Chemistry, Part II: Techniques for the Study of Biological Structure and Function*; W. H. Freeman: New York, 1998; pp 455–459.
- (25) Similar results were obtained at other wavelengths, with the anisotropy decaying from 0.40 to 0.012 with a lifetime of 61 fs at 688 nm and from 0.40 to 0.033 in 49 fs at 712 nm.
- (26) A slow rise phase with minor amplitude is apparent in the formation kinetics of the excited S₁ state of the tetrapyrrole at 701 nm following excitation of dyad **1** at 485 nm. There is an ~8 ps rise component in the region of the bleaching and stimulated emission of the Q_y band of the purpurin that can be attributed to the overlap of the carotenoid S₁ excited-state absorption, which has a tail extending at least as far as 730 nm (see Figure 7). The kinetics of dyad **1** display no slow rise component after subtraction of the decay kinetics of carotenoid **3** at 701 nm scaled by 26%. Instead, a recovery component of ~1.2 ps is revealed.
- (27) Liddell, P. A.; Nemeth, G. A.; Lehman, W. R.; Joy, A. M.; Moore, A. L.; Bensasson, R. V.; Moore, T. A.; Gust, D. *Photochem. Photobiol.* **1982**, *36*, 641–645.
- (28) Debreczeny M. P.; Wasielewski, M. R.; Shinoda, S.; Osuka, A. *J. Am. Chem. Soc.* **1997**, *119*, 6407–6414.
- (29) Theoretical predictions and experimental results suggest that another carotenoid excited singlet state lies between the S₁ and S₂ states.^{30,31} However, under the conditions of our experiments (temporal resolution, wavelength range, etc.), there is no evidence for the involvement of such a state in the singlet energy transfer process in **1**.
- (30) Tavan, P.; Schulten, K. *Phys. Rev. B* **1987**, *36*, 4337–4358.
- (31) Sashima, T.; Koyama, Y.; Yamada, T.; Hashimoto, H. *J. Phys. Chem. B* **2000**, *104*, 5011–5019.
- (32) Macpherson, A. N.; Gillbro, T. *J. Phys. Chem.* **1998**, *102*, 5049–5058.
- (33) If the ~1% reduction in the S₁ lifetime is the result of energy transfer and the formation yield of the S₁ state is 0.27, the contribution of the S₁ energy pathway (Figure 1) to the overall efficiency is negligible (~0.3%).
- (34) Engelman, R.; Jortner, J. *Mol. Phys.* **1970**, *18*, 145–164.
- (35) Wasielewski, M. R.; Johnson, D. G.; Bradford, E. G.; Kispert, L. D. *J. Chem. Phys.* **1989**, *91*, 6691–6697.

- (36) Andersson, P. O.; Bachilo, S. M.; Chen, R.-L.; Gillbro, T. *J. Phys. Chem.* **1995**, *99*, 16199–16209.
- (37) Onaka, K.; Fujii, R.; Nagae, H.; Kuki, M.; Koyama, Y.; Watanabe, Y. *Chem. Phys. Lett.* **1999**, *315*, 75–81.
- (38) Freer, A.; Prince, S.; Sauer, K.; Papiz, M.; Hawthornthwaite-Lawless, A.; McDermott, G.; Cogdell, R.; Isaacs, N. W. *Structure* **1996**, *4*, 449–462.
- (39) Kühlbrandt, W.; Wang, D. N.; Fujiyoshi, Y. *Nature* **1994**, *367*, 614–621.
- (40) Walla, P. J.; Yom, J.; Krueger, B. P.; Fleming, G. R. *J. Phys. Chem. B* **2000**, *104*, 4799–4806.
- (41) Gradinaru, C. C.; van Stokkum, I. H. M.; Pascal, A. A.; van Grondelle, R.; van Amerongen, H. *J. Phys. Chem. B* **2000**, *104*, 9330–9342.
- (42) Croce, R.; Müller, M. G.; Bassi, R.; Holzwarth, A. R. *Biophys. J.* **2001**, *80*, 901–915.
- (43) Macpherson, A. N.; Paulsen, H.; Gillbro, T. *PS2001 Proceedings: 12th International Congress on Photosynthesis; CSIRO Publishing: Melbourne, Australia, 2001; paper S31–025.*
- (44) Knox, R. S. *J. Photochem. Photobiol. B: Biol.* **1999**, *49*, 81–88.
- (45) Förster, T. *Ann. Phys.* **1948**, *2*, 55–75.
- (46) Nagae, H.; Kakitani, T.; Katoh, T.; Mimuro, M. *J. Chem. Phys.* **1993**, *98*, 8012–8023.
- (47) Damjanović, A.; Ritz, T.; Schulten, K. *Phys. Rev. E* **1999**, *59*, 3293–3311.
- (48) Dexter, D. L. *J. Chem. Phys.* **1953**, *21*, 836–860.
- (49) Scholes, G. D.; Fleming, G. R. *J. Phys. Chem. B* **2000**, *104*, 1854–1868.
- (50) For a model carotenoid and bacteriochlorophyll stacked face-to-face 3.5 Å apart, rates as high as $(0.14 \text{ ns})^{-1}$ can be calculated.⁴⁶ The rate drops to $(1.4 \text{ ns})^{-1}$ for a lateral displacement of 10 Å.
- (51) Gust, D.; Moore, T. A.; Luttrull, D. K.; Seely, G. R.; Bittersmann, E.; Bensasson, R. V.; Rougée, M.; Land, E. J.; de Schryver, F. C.; Van der Auweraer M. *Photochem. Photobiol.* **1990**, *51*, 419–426.
- (52) Freiberg, A.; Timpmann, K.; Lin, S.; Woodbury, N. W. *J. Phys. Chem. B* **1998**, *102*, 10974–10982.